

Experiment: Detecting Single Quantum Objects

In 1952, E. Schrödinger, one of the fathers of quantum mechanics and a Nobel Prize winner, wrote [160]:

We never experiment with just one electron or atom or (small) molecule. In thought experiments, we sometimes assume that we do; this invariably entails ridiculous consequences.

In 2012, S. Haroche and D. Wineland were awarded the Nobel prize

... for ground-breaking experimental methods that enable measuring and manipulation of individual quantum systems, according to the Nobel committee citation.

The juxtaposition of these two statements illustrates the tremendous progress of the experimental techniques in 60 years. They have allowed physicists to progress from gedanken experiments to feasible experiments. It also highlights the conceptual change that this progress induced. Physicists are now able to investigate the consequences of the single particle experiments envisioned by Schrödinger, but also to harness them to develop applications that are now known as quantum technologies.

With the exception of high energy physics experiments, for which the energy of the particles is so high that a single particle provides measurable macroscopic effects, like bubble formation, at Schrödinger time, most measurements were made on samples containing macroscopic quantities of quantum objects, of the order of the Avogadro number. For these experiments, the relevant quantities in the quantum mechanical description of the studied systems are *ensemble averaged quantities*, i.e. mean values, and sometimes variances and correlations. This approach has led to great successes, in particular the ab initio determination, from a quantum description of the microscopic world, of the value of many macroscopic parameters such as thermal and electrical conductivity, light absorption and scattering parameters.

The situation has evolved with the development over the years of increasingly sophisticated and sensitive experimental techniques: it is now possible to measure various properties of single quantum systems having an energy at the electron Volt level or even at the meV level: single atoms, ions, molecules, or photons are now the object of experimental studies. This allowed physicists to investigate new properties of the quantum world that may look strange or paradoxical (hence the word ridiculous used by Schrödinger), because they are far away from our intuition based on the macroscopic world. Nowadays, there are many experimental techniques

permitting to detect and manipulate single low energy quantum systems. In the remainder of this chapter, we give some examples of these techniques.

1.1 Destructive Detection of a Single Photon

A first category of photodetectors is based on the photoelectric effect: a photon that hits their surface has some probability to expel from it an electron that is then free. In photomultipliers the ejected electron is accelerated and hits another metallic surface from which it expels several electrons. The avalanche process is repeated several times and gives rise at the end of the series of metal surfaces to a macroscopic bunch of electrons, with a gain of up to 10^8 . This avalanche process produces a measurable pulsed electric signal that we call it a “click”. It witnesses the arrival of a single photon. Channel electron multipliers, or channeltrons, are similar devices that are able to deliver a macroscopic electric pulse from a single incident electron.

Photomultipliers need vacuum to operate. Most convenient devices are the solid-states avalanche photodiodes, made of a semiconductor junction. The photon incident on it creates an electron-hole pair. An avalanche process taking place in the high field region of the junction produces an electrical current in the external circuit. If the detector operates above the breakdown voltage (Geiger mode), the gain can be very high, of the order of 10^9 , so that a single photon gives rise to a measurable pulse with a high probability (up to 70%).

Bolometers constitute a second category of photodetectors. They record the temperature rise of an opaque body due to the absorption of light energy. Some of them are able to measure very high luminous powers. Others are extremely sensitive to very weak powers. The best ones consist of superconducting thin (5 nm) and narrow (100 nm) nanowires of very small heat capacity and cooled to very low temperatures: they are able to detect the transition from superconductivity to normal conduction induced by the heating induced by the energy carried by a single photon in the visible or infrared range! They give the same pulse height when more than one photon is present, so that they do not count the number of photons impinging on the detector, but detect only the presence of at least one photon.

Other kinds of superconducting devices, called transition edge sensors (TESs), are able to give different signals when 1, 2, 3 ... photons are incident on the detector (see Figure 1.1): they are called photon number resolving detectors [126]. They have a negligible dark count and a very high quantum efficiency, up to 90% that can be optimized in a wide spectral range, from mm waves to X-rays. They also have defects: they are slow and require a dilution refrigerator to operate.

Using more than one photon detector allows physicists to extract more information: with two detectors, one has access to photon correlations by *photon coincidence measurements*, which are of paramount importance in quantum physics (Section F.5); with the help of linear arrays of

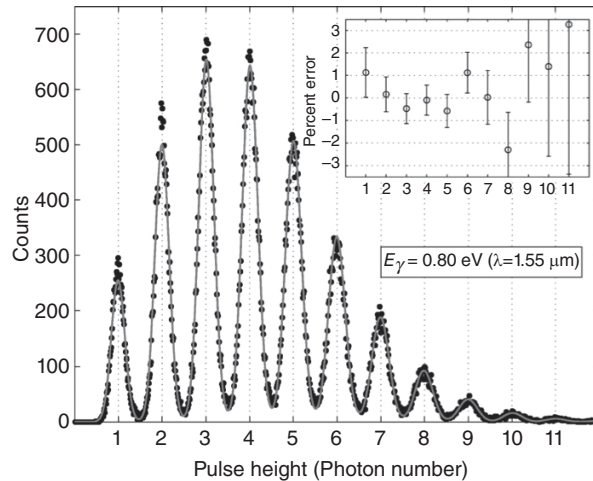


Fig. 1.1

Measured pulse-height distribution of a very weak laser pulse in a coherent state containing an average photon number of four photons using a superconductor calorimetric photon counter. The signals corresponding to 1–9 photons are well resolved. From A. Miller et al. Demonstration of a low-noise near-infrared photon counter with multiphoton discrimination, *Applied Physics Letters*, 2003. Reprinted from [126] with the permission of AIP.

photodiodes, or of charge coupled devices (CCD cameras) that are sensitive to single photons, experimentalists have access to the 1D or 2D position of the recorded single photons.

Electron multipliers and semiconductor devices are also sensitive to other kinds of incident particles, provided these particles bring an energy larger than the work function of the metallic electrode, or the energy gap of the semiconductor. This is, for example, the case of helium atoms. They can be easily detected individually when they are excited to the metastable state because of its high energy (20 eV). These atoms can also be precisely localized using a microchannel plate, which is an array of channeltrons.

1.2 Nondestructive Detection of the Presence of a Single Trapped Particle

Appropriate configurations of electric and magnetic fields, described in Appendix J, are able to create a harmonic potential around a chosen point \mathbf{r}_0 of the empty space so that a charged particle, like an electron or an ion, feels in its neighborhood a restoring force towards \mathbf{r}_0 likely to trap single electrons or ions.

Trapped charged particles, as any moving charged objects, induce currents in the electrodes. This current can be detected and witnesses the presence of the particle without destroying it. These induced currents are damped by the circuit's electrical resistance. This constitutes a relaxation process for the particle that efficiently reduces its energy in the trap. Because

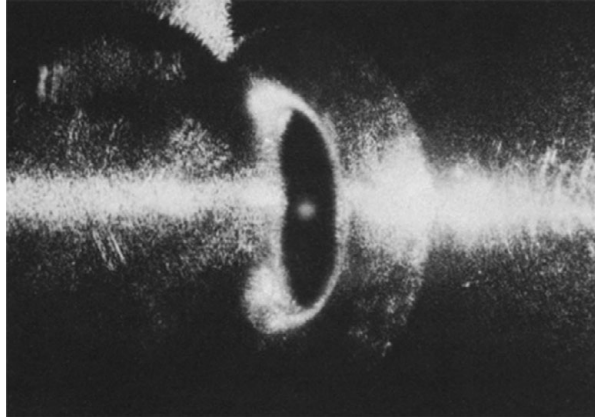


Fig. 1.2

One of the first photos ever of a single ion, which could be also seen by the naked eye. The small spherical cloud at the center of the photo is the image of the light scattered by the single Ba ion, whereas the surrounding light is the light scattered by the close-by trapping electrodes. From W. Neuhauser et al. Visual observation and optical cooling of electro-dynamically contained ions, *Applied Physics*, 1978 [135].

of collisions with other particles present in the evacuated chamber in which the experiment is made, the charged particles can be expelled one by one from the trap. Their number in the trap decreases with time, and can be equal to exactly one during a time that ranges from seconds to days or even months.

To measure the presence of the single trapped ion, one shines on the point \mathbf{r}_0 a laser beam that is resonant on the transition linking the ion ground state $|G\rangle$ to an excited state $|B\rangle$ of short lifetime T : the laser light excites the ion to level $|B\rangle$, which then decays back to $|G\rangle$ by emitting a spontaneous emission photon in a random direction: this is the well-known phenomenon of fluorescence. A proportion of these photons are collected by a large aperture lens and monitored on a photodetector. Due to the continuous laser irradiation the particle is quickly excited back to $|G\rangle$, and the cycle can be repeated. The flux of photons is thus of the order of 1 photon per lifetime, i.e. typically 10^8 photons per second for a 10 ns lifetime. This is an easily detectable bunch of photons, even by the naked eye: it is possible to actually see and to take a picture of a single ion. Figure 1.2 shows the fluorescence of a single Ba^+ ion. Note that the recorded fluorescence spot has a diffraction limited size of the order of the wavelength ($1\ \mu\text{m}$), which is much bigger than the ion size itself (roughly 50 pm).

The dipole force, described in Section J.1, induced by a highly focused off-resonant intense laser, provides a trap for polarizable objects like atoms. As with ions, a single atom can be detected by its fluorescence induced by another laser beam resonant on a closed transition, which is able to give rise to a large number of fluorescent photons. The fact that the trapping is due to a laser beam and not to fixed electrodes adds a lot of flexibility: using laser standing waves one can create an optical lattice of periodically disposed traps (Section 3.4 and Figure 1.3). Arrays of single atoms, candidates to be quantum registers for qubits, can also be produced in this way.

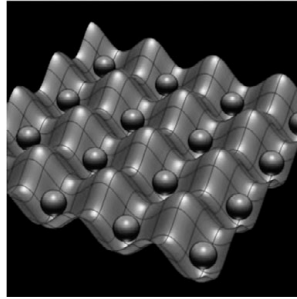


Fig. 1.3

Spatial shape of the dipole force potential experienced by atoms and created by interfering laser beams. Atoms are trapped at the periodic minima of this potential. From M. Takamoto et al. An optical lattice clock, *Nature*, 2005 [166].

1.3 Nondestructive Detection of the Energy Level of a Single Trapped Particle

Let us now describe a technique used to monitor in a nondestructive way, not only the presence of a single particle, but also its energy level. It is called the shelving technique, which can be used with ions and atoms as well.

We consider a three-level particle, which has a second excited state $|D\rangle$, that has a very long lifetime, in the configuration sketched in Figure 1.4. If the particle is in the ground state $|G\rangle$, a laser, resonant on the transition $|G\rangle \rightarrow |B\rangle$, will induce a strong fluorescence, as explained in Section 1.2, which can be easily recorded. If some process excites the atom to the level $|D\rangle$ (for example a weak lamp illumination), the cycle stops immediately and the fluorescence signal drops to zero. So the level of fluorescence is a direct measurement of the energy of the particle.

Figure 1.5 shows one example of a temporal sequence of the fluorescence signal from a single ion: its switch-off indicates a passage from $|G\rangle$ to $|D\rangle$ due to some excitation process whereas its switch-on indicates a passage from $|D\rangle$ to $|G\rangle$ due to spontaneous emission. The fluorescence signal of Figure 1.5 is characterized by the presence of on- and off- switches that occur randomly. They are the famous and fascinating *quantum jumps* that are distinctive features of the behavior of single quantum objects. *The exact time of such jumps cannot be controlled or predicted* by the experimentalist, to his great despair, as the main aim of physicists is to find ways to predict all physical phenomena. We will consider these quantum jumps in more detail in Section 4.5.

It is possible to record over very long times fluorescence signals that display many on- and off-quantum jumps. From this recorded data one can build the histogram of the dwell times t_D in the excited state $|D\rangle$ (Figure 1.6). This histogram can be fit by an exponential function, $e^{-t_D/T}$, which yields the lifetime T of the excited state $|D\rangle$. We see in this simple experimental example the very root of quantum physics: even though a

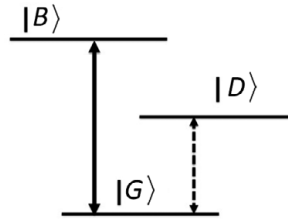


Fig. 1.4

Three-level particle (ion or atom) submitted to a laser light resonant with the transition $|G\rangle \rightarrow |B\rangle$ ("bright transition") producing a detectable fluorescent signal, and to a weak incoherent light resonant with the transition $|G\rangle \rightarrow |D\rangle$ ("weak transition").

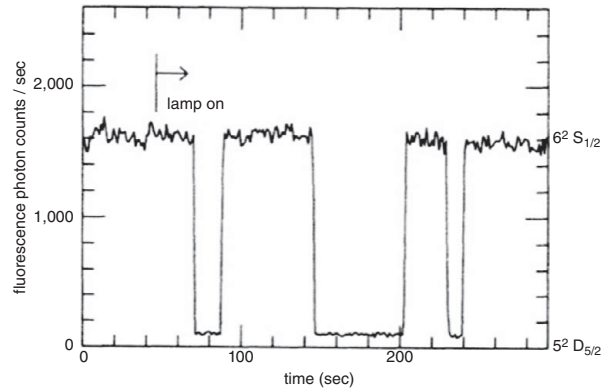


Fig. 1.5

Fluorescent signal emitted by a single ion submitted to a strong resonant laser field and a weak incoherent pumping light. The sudden changes in the signal reveal the *quantum jumps* experienced by the ion. From W. Nagourney et al. Shelved optical electron amplifier: Observation of quantum jumps, *Phys. Rev. Letters*, 1986 [132].

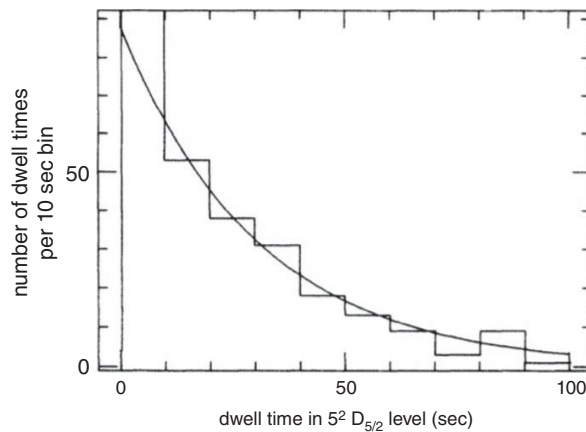


Fig. 1.6

Histogram of times spent in the excited state $|D\rangle$ (dwell times) corresponding to the periods of switched-off fluorescence in Figure 1.5. From W. Nagourney et al. Shelved optical electron amplifier: Observation of quantum jumps, *Phys. Rev. Letters*, 1986 [132].

single event on a single quantum object occurs randomly and cannot be predicted, the analysis of many successive single particle events allows us to accurately retrieve its properties such as its lifetime. This parameter could also have been directly measured on the fluorescence signal from a macroscopic sample of particles.

1.4 Destructive Detection of the Energy Level of a Single Atom

Highly excited states of atoms called Rydberg states (with high principal quantum numbers n , of the order of 50) have the interesting property that they can be counted one by one because their valence electron is weakly bound to the atomic core: an electrostatic field of 100 V/cm is enough to overcome the binding Coulomb field of the atomic core and therefore to ionize it: this is the field ionization phenomenon, which cannot be used for low-lying levels because it requires huge electrostatic fields for these levels. The ejected electron can then be individually counted by an electron multiplier, or channeltron.

To detect the presence of less excited atoms than Rydberg states, field ionization can be replaced by a suitable laser irradiation that is able to photo-ionize the atom.

The field ionization technique can even be used to distinguish atoms in Rydberg states with different quantum numbers n using the fact that

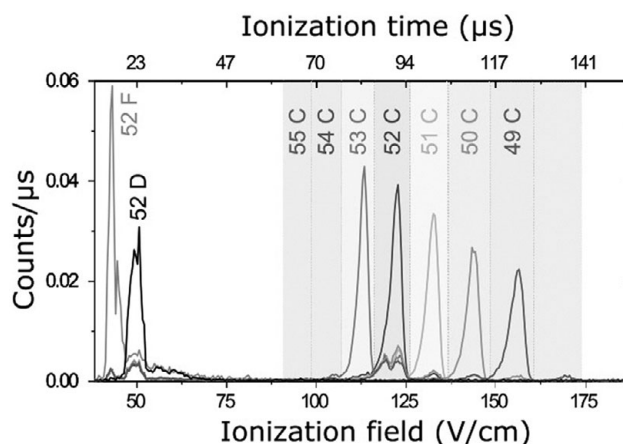


Fig. 1.7

ionization spectrum of single highly excited rubidium atoms, which are prepared in different circular states of principal quantum number ranging from 49 to 54. The ionizing field increases with time and the different levels, ionized for different values of the field, appear well separated: for well chosen values of the ionizing field, one circular level can be ionized and the next one not. From T. Cantat-Moltrrecht et al. Long-lived circular Rydberg states of laser-cooled rubidium atoms in a cryostat, *Physical Review Research*, 2020 [32], CC BY 4.0.

the minimum electrostatic field needed to ionize such atoms varies with n (it is actually proportional to n^{-4}). The set-up is sketched in Figure 3.2 of Chapter 3. The atom excited to a Rydberg state $|e_n\rangle$ of principal number n travels in the vacuum of an evacuated chamber between the two plates of plane capacitors, inside which exists an electrostatic field that is just enough to ionize level $|e_n\rangle$ but not the more bound state $|e_{n-1}\rangle$. The level $|e_{n-1}\rangle$ is ionized when the atom travels in a second capacitor placed downstream, inside which exists a stronger electrostatic field that can ionize the atom when it is in state $|e_{n-1}\rangle$.

In Figure 1.7, the state-selective field-ionization signal for Rydberg atoms of principal quantum numbers around 50 is shown. The measurement is done by ramping up the voltage of the ionization electrode and recording in real time the ionization signal from single Rydberg atoms using a channeltron. One notes that each Rydberg level has a characteristic ionization feature that is well separated from the next one.

1.5 Nondestructive Detection of Single Particles on a Surface

It is possible to detect a single molecule in a dilute sample of molecules located on a surface. This is done by using confocal microscopy (Figure 1.8). It involves a highly focused excitation beam that induces the fluorescence of the molecule, and a confocal pinhole that rejects the out-of-focus light and selects a small detection region of the image plane. If the density of the molecules adsorbed on the surface is low enough, there is a significant probability that a single molecule is in the detection

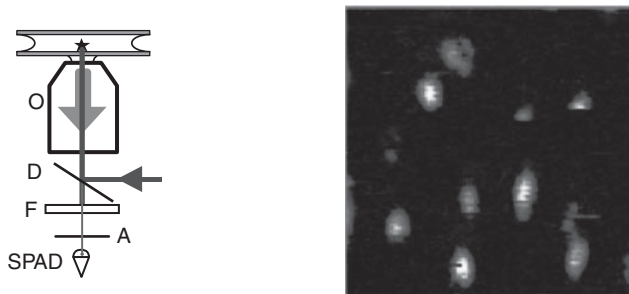


Fig. 1.8

(Left) Diagram of a confocal microscope. The sample to observe is at the top. O: high aperture objective; D: dichroic mirror transmitting the fluorescent light; F: filter; A: confocal aperture that restricts the axial extent of the observation volume; SPAD: single photon avalanche detector. (Right) Confocal image of isolated single molecules trapped on the surface (field: $10\ \mu\text{m} \times 10\ \mu\text{m}$). From W. E. Moerner and D. P. Fromm. Methods of single-molecule fluorescence spectroscopy and microscopy, *Review of Scientific Instruments*, 2003 [129].

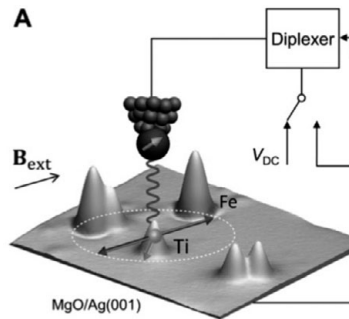


Fig. 1.9

Diagram of a STM imaging set-up: Ti atoms are individually positioned on a metallic surface with the help of the metallic tip of a scanning tunneling microscope. The spin states of these atoms are coherently manipulated at the single atom level by the tip playing the role of a microwave antenna. From Kai Yang et al. Coherent spin manipulation of individual atoms on a surface, *Science*, 2019 [181]. CC BY 4.0.

area. The laser beam is scanned over the surface, and searches for the location of the molecule on the surface. Usually, there are still many other background species in the detection area. One eliminates their fluorescence by the selective resonant character of the excitation of the desired molecule. It is often necessary to cool down the sample in order to get narrow enough transition linewidths and reduce the migration of the molecule.

In conventional spectroscopy, the inhomogeneity of the environment of the molecules located at different places induces a broadening of the transition called *inhomogeneous broadening*. This is not the case for single molecule spectroscopy, as there is no longer an ensemble averaging. The inhomogeneity now translates into a position-dependent shift of the resonance frequency, from one detected single molecule to another.

Single particles atoms lying on the surface of a solid can be also detected by scanning tunneling microscopy (STM), which allows us to scan a metallic surface with a nanometric resolution and detect single atoms that are adsorbed on it. By changing the voltage applied to the cantilever electrode that explores the surface, one can create a force that is sufficient to attach a chosen atom to the cantilever, to remove it from the surface and transport it to another chosen location, always with a single atom resolution. Figure 1.9 shows an STM image of Ti and Fe isolated atoms on MgO. The cantilever tip senses the different Ti spin orientations and their quantum superpositions. They constitute magnetic qubits that can be controlled by the microwave field emitted by the cantilever tip.

1.6 Quantum Jumps in Superconducting Circuits

Superconducting circuits are objects of several millimeters in size that can easily be seen with bare eyes (Figure 1.10) and look very classical.

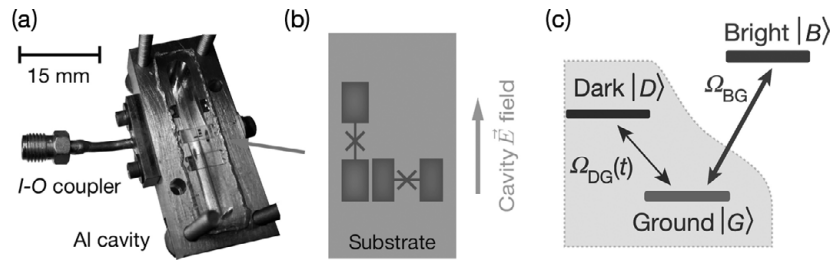


Fig. 1.10

(a) Experimental set-up used in the experiments from [185]. An aluminium cavity provides the high-Q superconductive environment. (b) A pair of artificial atoms (transmons on a sapphire chip) creates an artificial three-level molecule (c) used in the same way as the three-level system in ion jumps (Section 1.3). With permission from Z. Mineev. *Catching and Reversing a Quantum Jump Mid-Flight*, PhD thesis, Yale University, 2019 [185].

They are indeed macroscopic objects acting as microwave antennas. These antennas produce a microwave field that can be measured with ordinary electronics and usual data processing techniques. Nonetheless, as described in Appendix K, they can be brought to a fully quantum regime where they admit a description in terms of a single pair of conjugate quantum variables ruled by the Schrödinger equation [24, 133]. Just as with atoms, one can neglect their many-body “subatomic” structure in their description and treat them like indivisible quantum objects [55], hence their nickname “artificial atoms.” Their control and use is possible thanks to the Josephson tunnel junction, a nonlinear circuit element that is nondissipative and exhibits strong nonlinearity at the single photon level [56]. The nonlinearity allows the isolation of the two lower levels of an otherwise harmonic LC oscillator and their use as two-level systems [19]. Superconducting circuits can achieve a high quantum efficiency since the microwave environment can be engineered for the photons to leak through a single mode superconducting waveguide channeling them to an amplifier and subsequent detector. Thanks to the availability of cryogenic and microwave commercial technologies coherent Rabi and Ramsey oscillations (see Section G.3) are observed in these qubit systems with relative ease. With specially engineered quantum limited amplifiers the single quantum trajectories of these systems can be tracked, allowing quantum jumps to be observed in these macroscopic systems [171].

In Figure 1.10, we show a set-up [127] that was capable of observing quantum jumps in a macroscopic circuit imitating the “three level atom” already discussed in this chapter (see Section 1.3). Figure 1.10(a) shows the aluminium cavity with its microwave port (an SMA connector). A sapphire substrate with two aluminum artificial atoms, or “transmons” printed in orthogonal directions is in its interior and sketched in Figure 1.10(b) (see Appendix K). One of the transmons is aligned with the electromagnetic field of the fundamental mode of the cavity. This makes its antenna “bright” (B) since it can easily emit radiation into this mode. The other transmon is normal to the same electric field making it a “dark” (D) antenna which is weakly coupled to the fundamental mode. In Figure 1.10(c) we reproduce

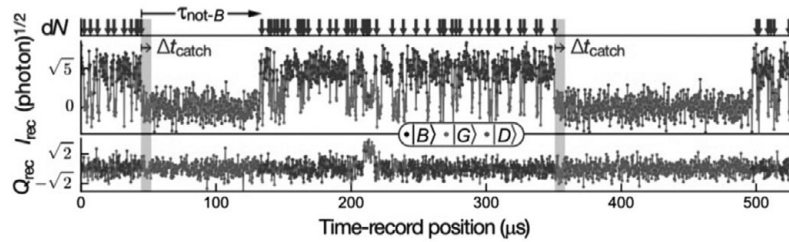


Fig. 1.11

Quantum jumps in a superconducting circuit experiment. Quadratures of the current I (middle recording) and charge Q (lower recording) of a probe microwave pulse are measured by homodyne detection to infer the state of the artificial atom. The vertical arrows of the upper recording correspond to “clicks” in the detection. The variable Δt_{catch} is the time period after the last “click” before a series of “no-clicks”. From Z. Mineev et al. To catch and reverse a quantum jump mid-flight, *Nature*, 2019 [127].

the three main levels of importance for this experiment. The ground state (G) is coupled to the bright state and to the dark state by two coherent drive fields. The field connecting to the bright state is strong and produces a fast Rabi oscillation, while the Rabi frequency towards the dark state is orders of magnitude weaker. The detection scheme relies on the fact that when the atom is in B state the frequency of the fundamental cavity mode (line width ~ 3 MHz) is dispersively shifted by ~ 5 MHz, and thus a probe field can provide information over the atomic state. This is reminiscent of a standard quantum optics measurement technique that is explained in detail in Appendix K: by measuring the quadratures of the reflected probe one can measure the resonance frequency of the resonator, which in turns reveals the atomic state in a quantum non-demolition way. Importantly in the experiment discussed, the D state is engineered to have a dispersive shift of ~ 0.3 MHz, making it indistinguishable from the signal corresponding to G . The binary measurement performed is then B , not- B . In Figure 1.11 we reproduce an experimental jump trace. The arrows in the top part of the panel represent “clicks” at the times at which the bright state is observed. Whenever that bright state is not detected the atom is most likely in the ground state and a sudden bright click is expected soon after. Rarely, though, the clicks are interrupted for a longer period corresponding to the atom visiting the dark state. After being “shelved” for a while in D a jump back to the ground state restarts the bright state “clicking.”

Even more remarkably, the high controllability offered by superconducting circuits allows us to highlight the difference in nature between the “up-jumps” (from G to D , during Δt_{catch} , see Figure 1.11) from the “down-jumps” (from G to D), events that were previously regarded jointly as discontinuous “jumps” [33, 48, 88]. We discuss this subject in more detail in Section 5.8.

1.7 Exercises for Chapter 1

- Exercise 1.1** Estimate the kinetic energy of a proton travelling at 99.999999% of the speed of light in the “high energy” particle accelerator. Why is it called “high energy” physics? Convince yourself that a mosquito (of mass ~ 10 mg) flying (at 1 m/s) in your room has a comparable kinetic energy.
- Exercise 1.2** “Low energy” experiments on single atoms or single ions experiments require laser cooling. Compute the mean kinetic energy and the velocity of Rubidium atoms at 1 μK . Compute the recoil velocity of a Rubidium atom after the absorption of a single $\lambda = 780$ nm photon.
- Exercise 1.3** Using that in the Bohr atomic model the radius of the n th orbit is $r_n = a_0 n^2$, show that the dependence of the ionization field for circular Rydberg atoms with the principal quantum number is n^{-4} .
- Exercise 1.4** What is the average number of photons in a ~ 51 GHz cavity if the environment is at 0.8 K? Compare to the expected value at room temperature. How is the argument modified for a resonator at 5 GHz?
- Exercise 1.5** The photon of Figure 3.3 was observed to live in the cavity during $T \sim 0.476$ s. The lifetime of the cavity was measured independently to be $T_{\text{cav}} \sim 0.13$ s. Compute the probability of observing a photon living during $\geq 0.476\text{s} \approx 3.7 \times T_{\text{cav}}$. What is the probability for a human to live 3.7 times (or more) its life expectancy? Discuss.